

Global MHD Simulation of the Earth's Magnetosphere Event on October, 1999

KYUNG SUN PARK, AND TATSUKI OGINO

Solar-Terrestrial Environment Laboratory Nagoya University, Toyokawa, Aichi 442-8507, Japan

(Received Oct. 4, 2001; Accepted Nov. 15, 2001)

ABSTRACT

The response of the earth's magnetosphere to the variation of the solar wind parameters and Interplanetary magnetic field (IMF) has been studied by using a high-resolution, three-dimension magnetohydrodynamic (MHD) simulation when the WIND data of velocity V_x , plasma density, dynamic pressure, B_y and B_z every 1 minute were used as input. Large electrojet and magnetic storm which occurred on October 21 and 22 are reproduced in the simulation (fig. 1). We have studied the energy transfer and tail reconnection in association with geomagnetic storms.

Key Words : method: IMF — magnetosphere — MHD

I. Introduction

We use a three-dimension global magnetohydrodynamic (MHD) model to simulation the interaction of the solar wind with the Earth's magnetosphere. The solar wind velocity, plasma density and pressure, and IMF B_y and B_z every 1-minute time resolution are need as input parameters. Characteristic of the solar wind dynamic pressure range from 1.8 nPa to 51 nPa and IMF B_z point southward for a long time with minimum of -31 nT. The analysis covers from 1200 UT on October 21 to 1200 UT on October 22, 1999 (fig. 2).

II. Simulation Method

We have solved the normalized resistive MHD and Maxwell's equation as an initial value problem by using a modified version of the Leap-frog scheme. The original version of MHD simulation model has described in detail by Ogino et al. [1992, 1994]. The MHD equations are the following:

$$\frac{\partial \rho}{\partial t} = -\vec{\nabla} \cdot (\vec{V} \rho) + D \nabla^2 \rho, \quad (1)$$

$$\frac{\partial \vec{v}}{\partial t} = -\vec{V} \cdot (\vec{\nabla} \vec{V}) + \frac{1}{\rho} \vec{\nabla} p + \frac{1}{\rho} \vec{J} \times \vec{B} + \vec{g} + \frac{1}{\rho} \mu \vec{\nabla}^2 \vec{V}, \quad (2)$$

$$\frac{\partial p}{\partial t} = -(\vec{V} \cdot \vec{\nabla}) p - \gamma p \vec{\nabla} \cdot \vec{V} + D_p \vec{\nabla}^2 p, \quad (3)$$

$$\frac{\partial \vec{B}}{\partial t} = \vec{\nabla} \times (\vec{V} \times \vec{B}) + \eta \vec{\nabla}^2 \vec{B}, \quad (4)$$

$$\vec{J} = \vec{\nabla} \times (\vec{B} - \vec{B}_d), \quad (5)$$

Where ρ is the plasma density, \vec{V} is the plasma flow velocity, p is the plasma pressure, \vec{B} is the magnetic field, \vec{B}_d is the main dipole field of the Earth, \vec{J} is the

current density, \vec{g} is the force of gravity, and γ is the ratio of specific heats with $\gamma = \frac{5}{3}$.

The simulation box has dimension of $30 \text{ Re} \leq X \leq -120 \text{ Re}$, $0 \text{ Re} \leq Y \leq 60 \text{ Re}$ and $0 \text{ Re} \leq Z \leq 60 \text{ Re}$, number of grid are $n_x, n_y, n_z = 500, 200, 400$ with a grid spacing of 0.3 Re. The mirror dipole field was used as an initial condition.

III. Simulation Result

1) When IMF turns from northward to southward which the four cell convection pattern changes to two cell convection pattern, convection is enhanced, the polar cap potential drop increases and onset of tail reconnection in plasma sheet, fast plasma flow on the tail is observed. 2) When IMF B_z becomes more southward and IMF B_y becomes more duskward, convection is enhanced and the energy flux decreases on the dayside, the polar cap potential drop increases. 3) When IMF B_z becomes more northward, IMF B_y reaches its peak value and dynamic pressure increases, the energy flux increases on the dayside and the polar cap potential drop remains constant that large value. 4) When IMF B_z becomes more northward, IMF B_y becomes less duskward and dynamic pressure increases, convection is reduced, the energy flux increases on the dayside and the polar cap potential drop remains constant. 5) For small changes in IMF and a large increases in dynamic pressure, convection is enhanced, the energy flux increases on the dayside and the polar cap potential drop decreases.

Response of the magnetosphere to solar wind is summarized in Table 1.

IV. Conclusions

1) Polar cap potential is dominated by IMF B_y as well as B_z ($\phi \approx 250 \text{ KV}$ for $B_z \approx -20 \text{ nT}$ and $\phi \approx 300 \text{ KV}$ for $B_z \approx -30 \text{ nT}$). Polar cap potential is saturated for strong southward IMF. 2) Polar cap potential maintains large value because IMF B_y has large value

Table 1. Response of the magnetosphere to solar wind

Time (UT)	
2300	Magnetospheric structure for northward IMF and four-cell convection pattern
2348	IMF turns from northward to southward
2355	Two-cell convection pattern and the cross polar cap potential has the minimum
0010	The cross polar cap potential drop increase
0012	Onset of tail reconnection
0018	Fast plasma flow in the tail (Expansion)
0119	Al index minimum (first step -1357 nT)
0259	The cross polar cap potential drop increases
0316	IMF Bz becomes more southward
0431	Al index minimum (second step -1992 nT)
0546	IMF By changed from negative to positive
0556	IMF Bz has the minimum value ($B_z = -31.5$ nT)
0630	IMF By has the maximum value ($B_y = 31.2$ nT)
0640	The cross polar cap potential has large values (~ 300 kV)
0700	Dst index minimum (- 231 nT)
0716	Solar wind dynamic pressure has the maximum value ($= 51.8$ nPa)

by rotation during increases IMF Bz. 3) Solar wind pressure enhancement has small effect to polar cap potential when IMF By and IMF Bz gradually decreases. 4) Bow shock closed to the earthward up to 8.3 Re, the distance of magnetopause is 5.4 Re and inner boundary of plasma sheet is -3.2 Re when the solar wind dynamic pressure reached the maximal 0700 UT.

ACKNOWLEDGEMENTS

The WIND data of the solar wind and magnetic field in ISTP key parameters was used courtesy of Drs. R. P. Lepping K. W. Ogilvie. AL, AU and Dst index data from WDC for Kyoto. Computing support was provided by the Computer Center of Nagoya University.

REFERENCES

Sonnerup. B.U. Ö., J. Geophys. Res., 79,1546,1974.
Taylor. J. B., physical. Rev. lett.,33,1139,1974
Ogino. T., J. Geophys. Res., 91,6791, 1986.
Ogino. T., R.J. Walker, M. Ashour-Abdalla., J. Geophys. Res., 99,11027,1994.
Raeder. J.,J. Berchem and M. Ashour-Abdalla., J. Geophys. Res., 103,14787,1998.

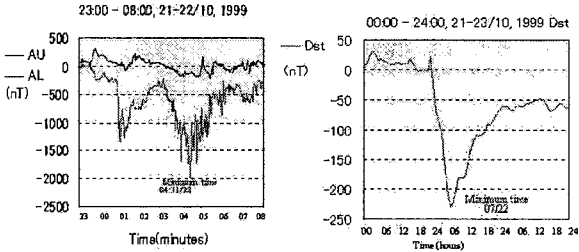


Fig. 1.— Large electro jet and magnetic storm which occurred fro October 21-22, 1999

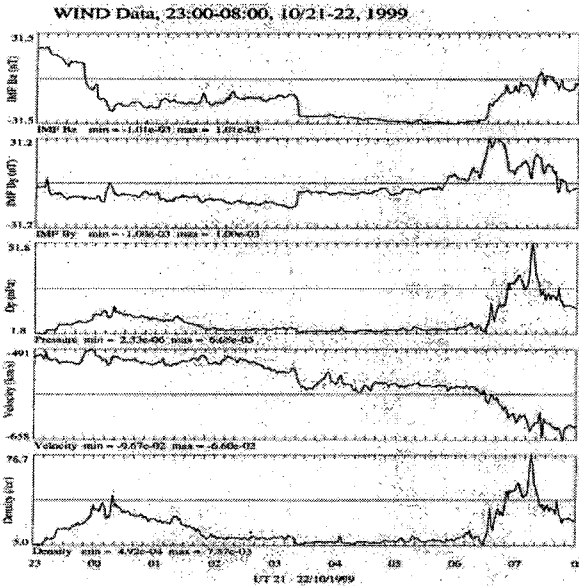


Fig. 2.— The WIND observations of the solar wind and IMF for 23:00 21/10 ~ 08:00 22/10

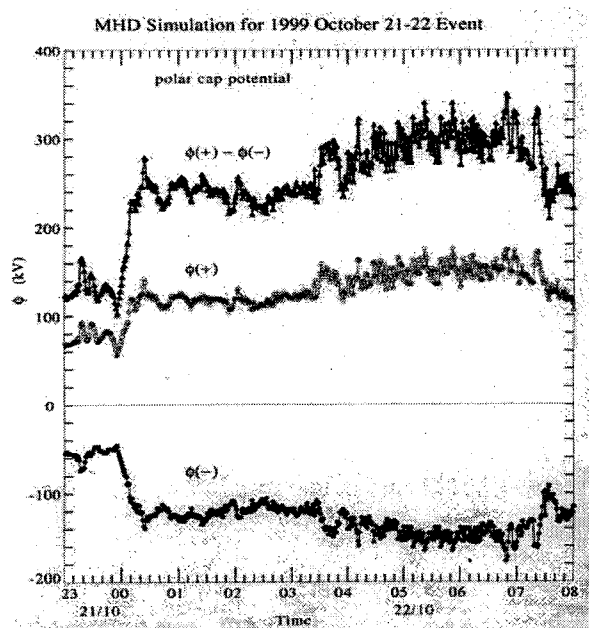


Fig. 3.— Time evolution of the simulation for the polar cap potential

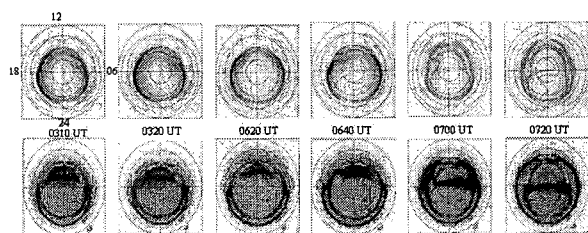


Fig. 4.— The time evolution of the potential and plasma convection in the polar region. Green line is open-closed boundary, red line is positive and blue line is negative

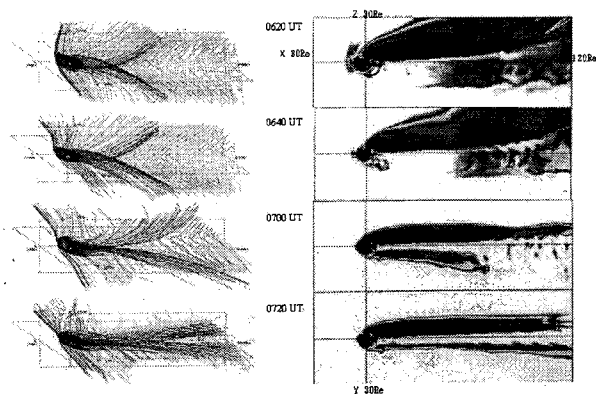


Fig. 5.— The time evolution of the magnetic field line and kinetic energy. Green line is closed, blue line is open and red line is detached